THE MATERIAL PROPERTIES OF HUMAN TIBIA CORTICAL BONE IN TENSION AND COMPRESSION: IMPLACATIONS FOR THE TIBIA INDEX

Andrew Kemper,
Craig McNally,
Eric Kennedy,
Sarah Manoogian,
Stefan Duma
Virginia Tech – Wake Forest, Center for Injury Biomechanics
United States
Paper Number 07-0470

ABSTRACT

The risk of sustaining tibia fractures as a result of a frontal crash is commonly assessed by applying measurements taken from anthropometric test devices to the Tibia Index. The Tibia Index is an injury tolerance criterion for combined bending and axial loading experienced at the midshaft of the leg. However, the failure properties of human tibia compact bone have only been determined under static loading. Therefore, the purpose of this study was to develop the tensile and compressive material properties for human tibia cortical bone coupons when subjected to three loading rates: static, quasi-static, and dynamic. This study presents machined cortical bone coupon tests from 6 loading configurations using four male fresh frozen human tibias. A servo-hydraulic Material Testing System (MTS) was used to apply tension and compression loads to failure at approximately 0.05 s^{-1}, 0.5 s^{-1}, and 5.0 s^{-1} to cortical bone coupons oriented along the long axis of the tibia. Although minor, axial tension specimens showed a decrease in the failure strain and an increase the modulus with increasing strain rate. There were no significant trends found for axial compression samples, with respect to the modulus or failure strain. Although the results showed that the average failure stress increased with increasing loading rate for axial tension and compression, the differences were not found to be significant. The average failure stress for the static, quasi-static, and dynamic tests were 150.6 MPa, 159.8 MPa, and 192.3 MPa for axial tension specimens and 177.2 MPa, 208.9 MPa, and 214.1 MPa for axial compression specimens. When the results of the current study are considered in conjunction with the previous work the average compressive strength to tensile strength ratio was found to range from 1.08 to 1.36.

INTRODUCTION

Lower limb injuries resulting from motor vehicle crashes are the second most common site of AIS 2+ injuri [27]. In addition, lower limb injuries have been reported to be a frequent cause of permanent disability and impairment [5]. Tibia and fibular shaft fractures account for 5% of AIS ≥ 2 lower extremity injuries and 8% of Life-years lost due to lower extremity injuries for front outboard occupants involved in frontal crashes [19].

The risk of sustaining tibia fractures as a result of a frontal crash is commonly assessed by applying measurements taken from anthropometric test devices to the Tibia Index (TI), developed by Mertz (1993). The Tibia Index, derived from combined stress analysis of a beam, is an injury tolerance criteria for combined bending and axial loading experienced at the midshaft of the leg:

$$TI = \frac{F}{F_c} + \frac{M}{M_c} \quad (1)$$

where F is measured compressive axial force (kN) in the superior-inferior direction, M is measured bending moment (Nm) in the leg, Fc is the critical force values, and Mc is the critical moment value. Mertz (1993) recommend critical force and moment values of 35.9 kN and 225 Nm, respectively. According to Mertz (1993), a TI reading less than 1 indicates that injury is unlikely. In order to protect against tibia plateau fracture, Mertz (1993) proposed a supplemental compressive force limit of 8 kN for the 50th percentile male dummy in addition to the Tibia Index formula.

Several authors have noted that the TI does not properly consider the combined effects of the two types of loading, because the TI assumes that the ultimate tensile strength and compressive strength of bone are equal [15, 26, 29]. Yamada (1970) reported that at static loading rates the ultimate compressive strength is approximately 1.08 times the ultimate tensile strength for human tibia compact, while Burstien and Reilly (1976) reported a slightly higher ratio of 1.25. Welbourne and Shewchenko (1998) illustrated that by arbitrarily increasing the TI injury threshold from 1 to 1.3 expands the injury boundary

to some extent. Currently the European Enhanced Vehicle Safety Committee (EEVC) for Euro NCAP uses the modified TI threshold of 1.3 as a compliance margin with the Hybrid III [19]. However, if maximum allowable force and moment values of 8 kN and 225 Nm are assumed, the TI is 1.223 [29]. Therefore, if the critical force and moment values are not increased by 30% to correspond with the increase in the TI threshold, the critical force and moment limits will always be exceeded before the TI reached 1.3 [29]. In addition, raising the threshold to 1.3 also changes the engineering basis of the TI, because the threshold of 1 is based on a standard engineering failure criterion [15]. Therefore, Funk et al. (2004) proposed a reformulated TI with revised critical values that accounts for effects tibia curvature and the differences in tensile and compressive strength while maintaining a threshold equal to 1. However, the ratio of compressive strength to tensile strength used by Funk et al. (2004) is based on a quasi-static data reported by Yamada (1970) for bone in general and not specifically for tibia cortical bone. Given that the properties of bone are rate dependant, the ability to accurately predict leg injuries could be improved by using a ratio of compressive strength to tensile strength for human tibia compact determined at a loading rate representative of that seen in automotive crashes [8, 21].

Although there have been numerous studies that have reported on the material properties of human tibia cortical bone in tension and compression, the research has been limited to static loading conditions and may not be representative of loading rates seen in automotive crashes. [7, 10, 12, 13, 31]. Therefore, the purpose of this study was to develop the matched tensile and compressive material properties for human tibia cortical bone coupons subjected to three loading rates, and determine the appropriate ratio to apply to the TI.

METHODS

This study presents 20 human tibia cortical bone coupon tests taken from the mid-diaphysis; 11 axial tension, 9 axial compression. The methodology is presented in four parts: experimental configuration, preparation of cortical bone coupons; testing configuration, detailing the MTS setup and measurement devices; and statistical methodology.

Subject Information

Tibia cortical bone specimens were dissected from two unembalmed fresh frozen male human cadavers. Freezing was used as a means to preserve the specimens because numerous previous studies have indicated that freezing does not significantly affect the material properties of cortical bone when frozen to a temperature of -20° C [14, 16, 17, 20, 25].

For comparison with the standard population, the bone mineral density (BMD) of each cadaver was determined by the Osteogram technique. The left hand of the cadavers was x-rayed, scanned and processed by CompuMed incorporated (Los Angeles, CA). This type of BMD measurement, however, only provides an indication of overall bone strength and does not account for local changes in bone density or composition. Therefore, the BMD obtained through this method is referred to as the "Global BMD". The global BMD results are reported with respect to the normal population (Table 1). The T-score is used to compare the cadaver's global BMD with that of the general population, using 30 years of age as the comparison. The Z-score is used to compare the global BMD of the subjects with the average for their age. A T-score of -1 corresponds to one standard deviation below the mean for the general population, meaning the individual is at or above the 63rd percentile for global BMD, or close to normal. T-scores of 2 and 3 correspond to 97th and 99th percentiles, respectively.

Specimen Preparation

In order to conduct material property testing on human cortical bone, the bone coupon must first be machined into a testable geometry. This was done through numerous steps of detailed preparation [18]. First, an oscillating bone saw was used to make two cuts to separate the tibia from the body (Figure 1, (Figure 2A).

Table 1. Osteogram data for cadavers used in tibia cortical bone testing.

Cadaver	Gender	Age	Global BMD	T-Score	Z-Score
Sm39	M	67	105.4	-0.5	0.9
Sm37	M	56	105.3	-0.5	0.3

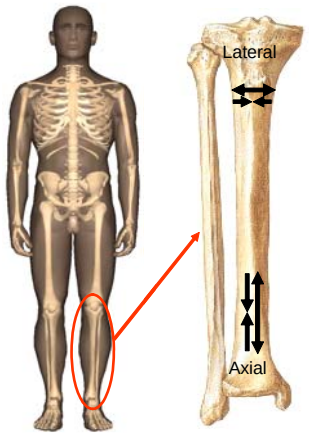

Figure 1. Isolated tibia showing axial and lateral specimen orientations.

The mid-diaphysis of the tibia was cut into sections using a low speed diamond saw with micrometer precision (Figure 2 B). The diamond saw blade was immersed a saline bath to minimize the heat created from friction and maintain specimen hydration, which has been shown to significantly affect the material properties, specifically plasticity, of cortical bone [6]. Then, the sections cut from the tibia were placed in a bone chuck and two parallel cuts were made along the longitudinal axis to remove a rectangular section of the bone (Figure 2 C). Great care was taken when placing the bone sections in a bone chuck to ensure that the axis axis of the tibia coincided with the axis of cutting. The rectangular cortical bone specimen was placed in a custom bone chuck, and a third cut was made to remove the cancellous bone from the piece (Figures 2 D and E). This cut also created a flat side that was placed faced down on the milling base. Finally, additional cuts were made to level the uncut side and, if necessary, trim the ends to fit on the milling base. It should be noted that the dimensions of the rectangular cortical bone specimens were cut slightly larger than the final specimen dimension to allow a clamping area for the milling process. Since the tibia is triangularly shaped, this process was repeated in order to obtain rectangular cortical bone specimens from all three sides of the tibia.

The resulting rectangular cortical bone specimen was then milled to the final test specimen dimensions using a small Computer Numerical Control (CNC) machine (MAXNC 10, MAXNC Inc., Chandler, AZ). A rectangular pocket was milled into a plastic milling base to create a surface parallel to the z-axis, or vertical axis, of the mill. The flat side of the rectangular cortical bone specimen was placed on the plastic milling base. This was done to assure that the top face of the cortical bone specimen was milled parallel to the flat face. Again, great care was taken when placing the cortical bone specimen on the milling base to ensure the axis of interest coincided with the axis of the mill. The milling base was placed in a saline bath to minimize heat and maintain specimen hydration. The mill ran two codes to cut the specimen to the final dimension with micrometer precision. The final test specimen dimensions were based on both previous literature and ASTM standards for tension and compression material testing [3, 4, 9, 10, 24, 21, 30, 32] (Figures 3 and 4). Finally the coupons were evenly sanded with 240, 320, 400, and 600 grit wet sand paper. The finished specimens were kept immersed in a saline solution and refrigerated until tested. Once the specimens were placed on the test setup, they were kept hydrated by spraying a saline solution on them.

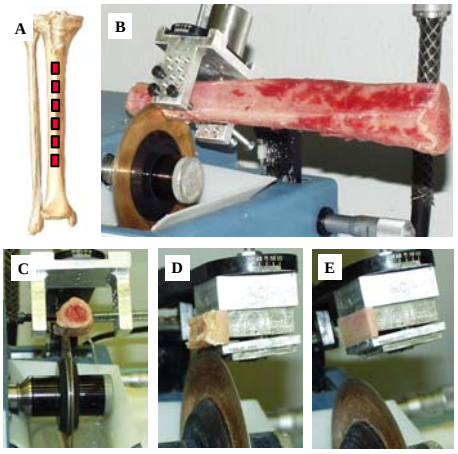

Figure 2. A) Isolate tibia. B) Mid-diaphysis divided into smaller sections. C) Parallel cuts along the long axis of the tibia D) Isolate the cortical bone from the cancellous bone. E) One flat side to place face down on the milling base.

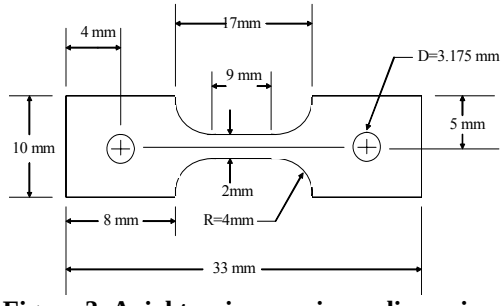

Figure 3. Axial tension specimen dimensions. Note: Specimen thickness = 2mm.

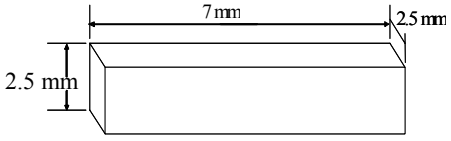

Figure 4. Axial compression specimen dimensions.

Testing Configuration

A high-rate servo-hydraulic Material Testing System (MTS) was used to apply either tension or compression loads to failure at approximately 0.05 s^{-1}, 0.5 s^{-1}, and 5.0 s^{-1} on the cortical bone coupons. For all failure tests, a 2224 N load cell was used to measured load (MTS 661.18E-02, 2224 N, Eden Prairie, MN). Displacement was measured with a laser vibrometer (Polytec, OFV 303, Tustin, CA).

A total of five displacement measurement devices were evaluated for accuracy under both static and dynamic loading conditions. The devices included: a strain gage, potentiometer, extensometer, laser vibrometer, and the MTS internal LVDT. The standard displacement measurement device for static material testing is an extensometer, which provides a direct displacement measurement of the specimen gage length. However, the grips of the extensometer slip during the high rate testing resulting in inaccurate displacement readings. Like the extensometer, a strain gage provides a direct displacement measurement of the specimen gage length. However, tests conducted with a strain gage applied over the specimen gage length showed a large reduction in ultimate stress and strain. This was due to localized specimen drying, required to apply the strain gage, which has been shown to significantly affect the material properties, specifically plasticity, of cortical bone [6]. The potentiometer is a non-contact displacement measurement device, which does not affect the properties of the material being tested. However, the potentiometer data did not show the same response time as the extensometer for slow rate tests. The MTS internal LVDT was found to have relatively poor resolution. Finally, the laser vibrometer, which has nanometer scale accuracy and a high frequency response of 200 kHz, showed almost the exact response as the extensometer at static and quasi static rates. Unlike the extensometer; however, the laser vibrometer also gives accurate readings during high rate testing.

For dynamic testing, the MTS actuator must travel a finite distance to reach the desired test speed. If the actuator is directly coupled to the test coupon, then a toe region will be seen in the stress vs. strain response. In order to avoid this, the use of a custom lack adapter was employed (Figure 5). A shaft with a male conical end rested inside a hollow tube with a female conical end, which was directly coupled to the MTS actuator. The MTS was programmed lift or lower the slack adapter tube, depending on the testing direction, to allow enough space to reach the desired speed before coming into contact with the slack adapter rod. Once the MTS reached the desired speed and engaged the slack adapter, the piece was loaded at a constant rate to failure. The slack adapter was designed to work in both tension and compression test configurations (Figure 5).

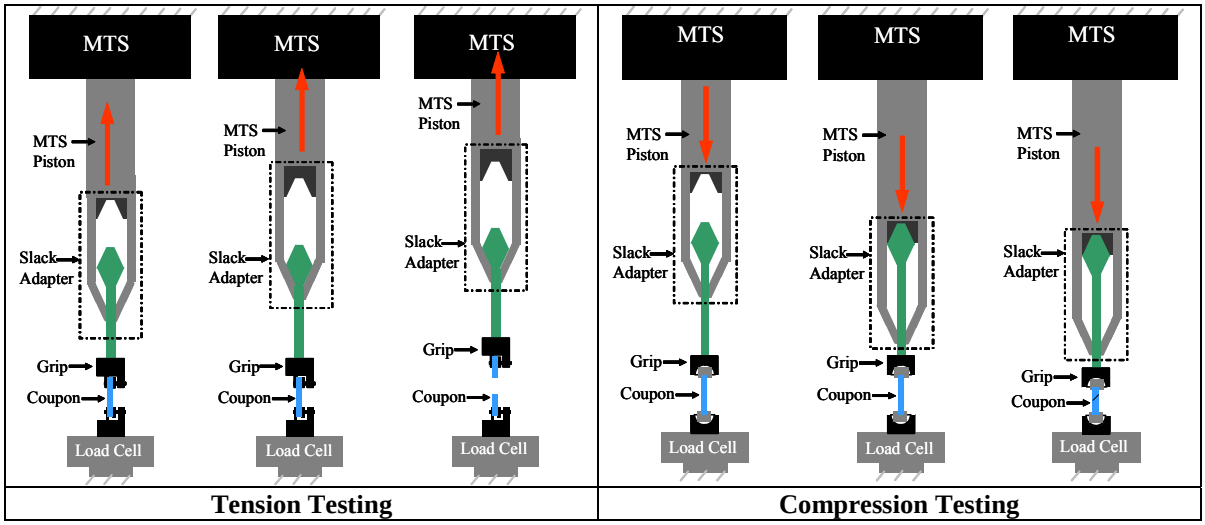

Figure 5. Slack adapter in test configurations.

Alignment of Test Setup

The three main sources of misalignment in a material testing setup were addressed in order to minimize variable bending stresses, which result in a reduction in both strength and ductility. As described earlier, extreme care was taken during the specimen preparation process to maintain symmetric machining along the axis of interest of the test specimens. The conformance of the specimen centerline to the top and bottom grip centerlines was addressed through design and precise machining of the grips. For tension testing, the grips were designed to use both a pin and clamp configuration. The pin ensured proper centerline conformance, and the clamp provided the holding force. To hold the bone coupon in place, the grip screws were tightened, forcing metal plates to clamp both ends of the coupon (Figure 6). For compression testing, proper centerline conformance was ensured by milling a 1 mm deep circular placement groove, concentric with the grip centerline, in the top and bottom loading surfaces (Figure 7). The diameter of the placement hole was such that the corners of the compression specimen just slightly cleared. In compression testing, it is critical that the two loading faces are parallel. In order to compensate for any angular misalignment of the compression grips or faces of the compression specimen, lubricated rotating hemispheres were placed on the top and bottom grips [4]. The compliance of the lubricant was taken into account by conducting a series of compression tests with no specimen in the grips. The resulting force verse displacement curves were then fitted and used to adjust the displacement data from the actual cortical bone compression tests. In order to align the centerlines of the top and bottom grips, an aluminum specimen with the same dimensions of the cortical bone coupon specimens was instrumented with strain gages on all four sides of the gage length [1]. A dial indicator read the position so the load cell could be adjusted in small increments until the strain gages read within 100 microstrain of one and other, which is less than 1 % of the total loading strain in the tests.

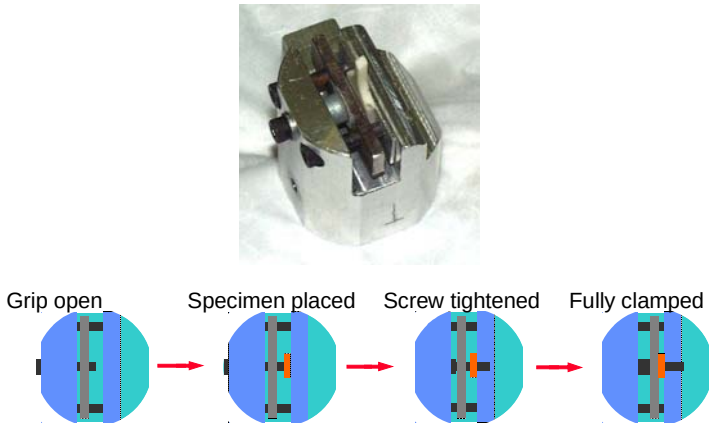

Figure 6. Tension test grips with pin and clamp design.

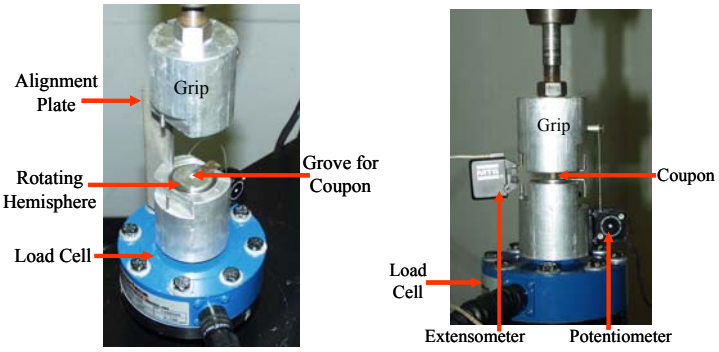

Figure 7. Compression test grips with centering groove to ensure proper centerline conformance.

Data Processing

The load and strain data were collected and filtered at different levels depending on the speed of each test (Table 2). Each filter class changed the peak stress and strain by less than 1%. Stress was calculated by dividing the force measurement by the cross sectional area of the specimen gage length. Strain was determined using the Lagrangian formulation of dividing the change in length by the initial length. The modulus of elasticity was defined as the slope between two points, approximately 30 % and 70 % of the yield point.

Table 2. Sampling frequency and CFC filter for each test series.

Strain Rate	Compression	Tension
0.05 s-1	15kHz/ CFC180	10kHz/ CFC180
0.5 s-1	30kHz/ CFC600	30kHz/ CFC600
5.0 s-1	100kHz/ CFC1000	100kHz/ CFC1000

Statistical Analysis

Statistical analysis was performed on all of the data in order to illustrate significant differences between the values for the 6 different groups of tests. For this analysis, multiple t-tests were performed between each group of data for each value. The Tukey-Kramer technique was used which adjusts for multiple comparisons. P-values are presented with statistical significance assigned to a p-value of 0.05 or less.

RESULTS

Tension tests were performed on a total of 11 human tibia cortical bone coupons at three stain rates. The tension mechanical properties for each specimen as well as averages by testing group are shown in Table 3. The average failure stress for the static, quasi-static, and dynamic tests were 150.6 MPa, 159.8 MPa, and 192.3 MPa for axial tension. The average failure strain for the static, quasi-static, and dynamic tests were specimens and 23696 microstrain, 19228 microstrain, and 18329 microstrain for axial tension specimens. The stress vs. strain curves for all tension tests are also shown (Figure 8).

Compression tests were performed on a total of 9 human tibia cortical bone coupons at three stain rates. The compression mechanical properties for each specimen as well as averages by testing group are shown in Table 4. The average failure stress for the static, quasi-static, and dynamic tests 177.2 MPa, 208.9 MPa, and 214.1 MPa for axial compression specimens. The average failure strain for the static, quasi-static, and dynamic tests were 16116 microstrain, 19587 microstrain, and 21198 microstrain for axial compression specimens. The stress vs. strain curves for all compression tests are also shown (Figure 9).

Table 3. Axial tension material properties.

Series	Test	Strain Rate (strains/s)	E (GPa)	Ultimate Strain (microstrain)	Ultimate Stress (MPa)
ATF	L1	0.045	19.15	25028	151.3
ATF	L2	0.041	18.89	23392	159.0
ATF	L3	0.044	19.33	24717	151.1
ATF	L4	0.055	16.04	21647	141.1
ATFL Average		***0.046***	***18.35***	***23696***	***150.6***
ATF	M1	0.656	15.56	20986	152.2
ATF	M2	0.464	19.18	18073	172.9
ATF	M3	0.629	16.35	19918	155.3
ATF	M4	0.586	17.86	17937	158.8
ATFM Average		***0.584***	***17.23***	***19228***	***159.8***
ATF	H1	5.077	29.88	18966	180.0
ATF	H2	7.336	41.95	21223	230.5
ATF	H3	5.669	30.76	14797	166.5
ATFH Average		***6.027***	***34.19***	***18329***	***192.3***
ATF Average		***2.167***	***22.27***	***20607***	***165.3***

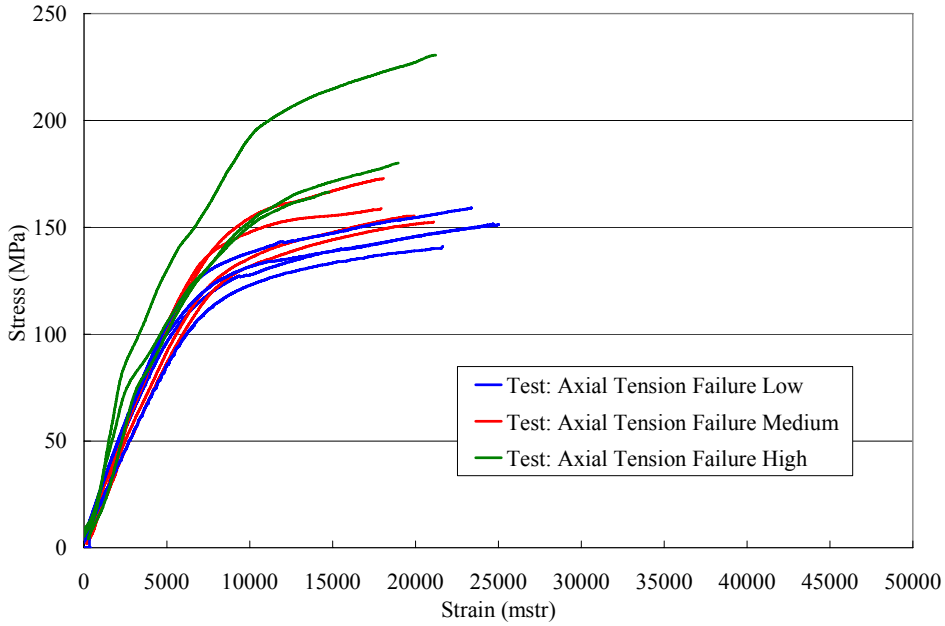

Figure 8. Axial tension static, quasi-static, and dynamic tests.

Table 4. Axial compression material properties.

Series	Test	Strain Rate (strains/s)	E (GPa)	Ultimate Strain (microstrain)	Ultimate Stress (MPa)
ACF	L1	0.043	18.86	15944	197.9
ACF	L2	0.044	13.63	18315	165.6
ACF	L3	0.039	18.23	14089	167.9
ACFL Average		***0.042***	***16.91***	***16116***	***177.2***
ACF	M1	0.580	16.03	20700	197.7
ACF	M2	0.464	19.58	16568	208.1
ACF	M3	0.453	18.53	21492	220.8
ACFM Average		***0.499***	***18.05***	***19587***	***208.9***
ACF	H1	4.874	12.82	16137	223.5
ACF	H2	4.591	13.67	22817	195.1
ACF	H3	3.667	13.53	24639	223.6
ACFH Average		***4.377***	***13.34***	***21198***	***214.1***
ACF Average		***1.640***	***16.10***	***18967***	***200.0***

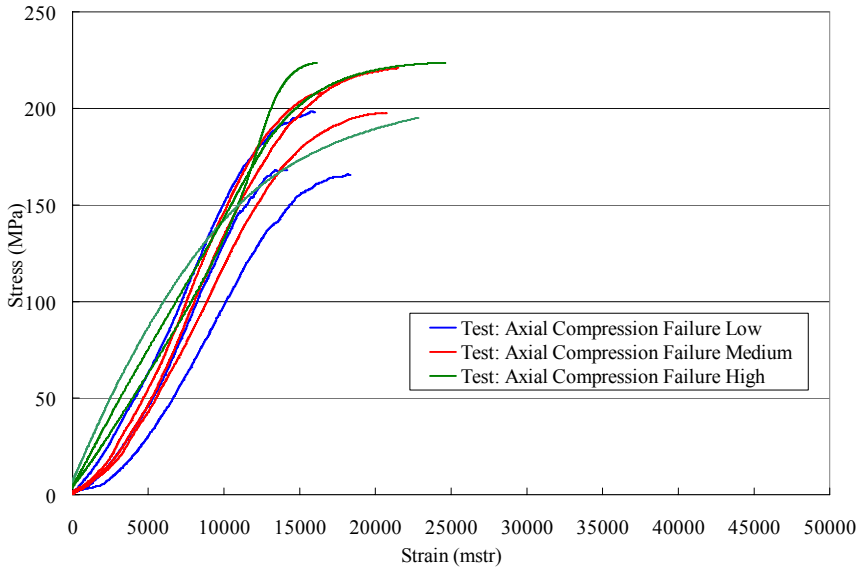

Figure 9. Axial compression static, quasi-static, and dynamic tests.

Statistical Analysis

Statistical analysis was performed on all of the data in order to illustrate significant differences between the values for the 6 different groups of tests. For this analysis, multiple t-tests were performed between each group of data for each value. The Tukey-Kramer technique was used which adjusts for multiple comparisons. P-values are presented with statistical significance assigned to a p-value of 0.05 or less (Tables 5-7). Although minor, axial tension specimens showed a decrease in the failure strain and an increase the modulus with increasing strain rate. There were no significant trends found for axial compression samples, with respect to the modulus or failure strain. Although the results showed that the average failure stress increased with increasing loading rate for axial tension and compression, the differences were not found to be significant.

Table 5. P-values for the elastic modulus (E) for all failure test groups.

	ACFH	ACFL	ACFM	ATFH	ATFL	ATFM
ACFH	*					
ACFL	0.9209	*				
ACFM	0.6789	0.9999	*			
ATFH	0.0001	0.0001	0.0001	*		
ATFL	0.4992	0.9999	0.9999	0.0001	*	
ATFM	0.8139	0.9999	0.9999	0.0001	0.9999	*

Table 6. P-Values for ultimate stress for all failure test groups.

	ACFH	ACFL	ACFM	ATFH	ATFL	ATFM
ACFH	*					
ACFL	0.4564	*				
ACFM	0.9999	0.6706	*			
ATFH	0.9564	0.9973	0.9945	*		
ATFL	0.0065	0.7972	0.0163	0.2062	*	
ATFM	0.0319	0.9861	0.0733	0.5436	0.9999	*

Table 7. P-Values for ultimate strain for all failure test groups.

	ACFH	ACFL	ACFM	ATFH	ATFL	ATFM
ACFH	*					
ACFL	0.8541	*				
ACFM	0.9999	0.9883	*			
ATFH	0.1297	0.9567	0.3464	*		
ATFL	0.9987	0.2661	0.9376	0.0094	*	
ATFM	0.9999	0.9916	0.9999	0.3210	0.8420	*

DISCUSSION

The static tensile material properties of human tibia bone presenting in this study were found to consistent with previously published material property data (Tables 8). The tensile modulus, average ultimate tensile stress, and average ultimate tensile strain data from the current study lie within the values reported by previous authors. The differences in reported material property values could be attributed to a number of variables know to influence the properties of bone: age, bone density, specimen hydration, or gender.

The static compressive material properties of human tibia bone presenting in this study were also found to consistent with previously published material property data (Table 9). The average compressive ultimate stress data from the current study lie within the values reported by previous authors. Burstein and Reilly(1976) and Evans and Vincentelli (1967) reported higher modulus values, 28.0 GPa and 19.3 GPa respectively, than the current study. However, Evans (1967) reported a lower average ultimate compressive strain value than the current study. Again, differences in reported material property values could be attributed to a number of variables know to influence the properties of bone: age, bone density, specimen hydration, or gender.

.

Table 8. Comparison of reported human tibia compact bone material properties in axial tension.

Author	Age	Loading Rate	Modulus (GPa)	Ultimate Strain (microstrain)	Ultimate Strength (MPa)
Dempster (1961)	N/R	N/R	N/R	N/R	95.3
Melick (1966)	N/R	N/R	N/R	N/R	138.3
Evans (1967)	33-98	N/R	15.2	16500	97.1
Yamada (1970)	20-39	N/R	18.0	15000	140.3
Burstein (1976)	50-59	0.05 s-1	23.1	31000	164.0
Kemper (2004)	56-67	0.046 s-1	18.4	23696	150.6

Table 9. Comparison of published human tibia compact bone material properties in axial compression.

Author	Age	Loading Rate	Modulus (GPa)	Ultimate strain (microstrain)	Ultimate strength (MPa)
Yamada (1970)	20-39	N/R	N/R	N/R	151.1
Burstein (1976)	50-59	0.05 s-1	25.1	N/R	183.0
Evans (1974)	26-75	0.045 in/min	19.3	9510	109.0
Kemper (2007)	56-67	0.042 s-1	16.4	16116	177.2

Although there have been numerous studies that have reported on the material properties of human tibia cortical bone in tension and compression, only two have conducted matched tension and compression testing [7, 31]. The ratio of compressive strength to tensile strength from these studies was compared with the results from the current study (Table 10). In the current study, the ratio of compressive strength to tensile strength ranged static, quais-static, and dynamic test groups were 1.17, 1.31, and 1.11 respectively. However, given that there where no significant differences found in ultimate stress by loading rate in the current study, all three loading rate groups where used in to determine an average ratio of compressive strength to tensile strength of 1.21. Burstein and Reilly (1976) reported ultimate stress grouped by age. Therefore, a ratio of compressive strength to tensile strength was calculated for each age group, and ranged from 1.15 to 1.36. The average of all the age groups reported by Burstein (1976) was found to be 1.24.

Welbourne and Shewchenko (1998) illustrated that arbitrarily increased the TI injury threshold to 1.3, to account for the differences in compressive strength and tensile strength increases the injury boundary somewhat. However, Welbourne and Shewchenko (1998) also showed that based on the maximum allowable force and moment values proposed by Mertz (1993) the highest TI value is 1.223. Consequently, the modified TI threshold of 1.3 currently used by the European Enhanced Vehicle Safety Committee (EEVC) for Euro NCAP is too high. Funk et al. (2004) used a ratio of 1.2 a reformulated TI formula with revised critical force and moment values, which take both tibia curvature and difference in compressive strength and tensile strength into account, and showed increase the injury prediction over a ratio equal to 1. Although, the ratio of 1.2 was based on static data reported by Yamada (1970) for bone in general, the results of the current study show that 1.2 is a reasonable value for since it lies within the range of ratios for human tibia cortical bone determined at various loading rates.

Table 10. Comparison of tibia compressive strength to tensile strength ratios.

Author	**Age**	**Loading Rate**	$\frac{\sigma_{UT}(comp)}{\sigma_{UT}(ten)}$
Yamada (1970)	20-39	N/R	1.08
Burstein (1976)	20-89	0.05 s-1	1.24 (avg.) [1.15-1.36]
Kemper (2007)	56-67	0.04 to 7.3 s-1	1.21 (avg.) [1.17-1.31]

CONCLUSIONS

The material properties of human tibia cortical bone were determined from cortical bone coupons obtained from the mid-diaphysis at three different loading rates. The mechanical properties presenting in this study were found to be consistent with previously published data at similar loading rates. Therefore, the specimen preparation and test methods presented in this study are both accurate and precise for determining cortical bone material properties. Although minor, axial tension specimens showed a decrease in the failure strain and an increase the modulus with increasing strain rate. There were no significant trends found for axial compression samples, with respect to the modulus or failure strain.

Although the results showed that the average failure stress increased with increasing loading rate for axial tension and compression, the differences were not found to be significant.

When the results of the current study are considered in conjunction with the previous work the average compressive strength to tensile strength ratio was found to range from 1.08 to 1.36. Although the previously used ratio of 1.2 was based on static, the results of the current study show that it is a reasonable value for since it lies within the range of ratios for human tibia cortical bone determined at various loading rates.

ACKNOWLEDGMENTS

The authors wish to acknowledge Toyota Motor Corporation for providing the funding for this research

REFERENCES

[1] ASTM Standard E 1012-99, ASTM (2004). "Standard Practice for Verification of Specimen Alignment." American Society of Testing and Materials, Philadelphia, PA.

[2] ASTM Standard E 8M-01, ASTM (2004). "Standard Test Methods for Tensile Testing of Metallic Materials [Metric]." American Society of Testing and Materials, Philadelphia, PA.

[3] ASTM Standard D 5026-01, ASTM (2004). "Standard Test Methods for Plastics: Dynamic Mechanical Properties: In Tension." American Society of Testing and Materials, Philadelphia, PA.

[4] ASTM Standard E 9-89a, ASTM (2004). "Standard Test Methods of Compression Testing of Metallic Materials at Room Temperature." American Society of Testing and Materials, Philadelphia, PA.

[5] Burgess et al. (1995). "Lower Extremity Injuries in drives od Airbag-Equipped Automobiles- Clinical and Crash Reconstruction Correlations." J. of Trauma. 38, 509-516.

[6] Burstien, A.H., Reilly D.T., and Victor, H.F. (1972). "The Ultimate Properties of Bone Tissue: The Effect of Yielding." *J. Biomechanics*. 5, 35-44.

[7] BurstienTIEN, A.H., Reilly D.T., and Martens M. (1976). "Aging of bone tissue: Mechanical Properties." *Journal of Bone and Joint Surgery*. 58-A(1),82-86.

[8] Carter, D.R., and Haynes, W.C. (1976). "The Compressive Behavior of Bone as a Two-Phase Porous Structure." *J. of Bone and Joint Surgery*. 59-A, 954- 962.

[9] Crowninshield, R., and Pope M. (1974). "The Response of Compact Bone in Tension at Various Strain Rates." *Annals of Biomedical Engineering*. 2, 217-225.

[10] Dempster, W.T., and Lippicoat R.T. (1952). "Compact Bone as a Non-Isotropic Material." *Amer. J. Anat*. 91, 331-362.

[11] Dempster, W.T., and Coleman, R.F. (1961). "Tensile Strength of Bone Along and Across the Grain." *J. Appl. Physiol*. 16, 355-360.

[12] Evans F.G. and Vincentelli R. (1974). "Relations of the Compressive Properties of Human Cortical Bone to Historical Structure and Calcification." *J. Biomechanics*. 7, 1-10.

[13] Evans, F.G., and Bang, S. (1967). "Differences and Relationships Between the Physical Properties and Microscopic Structure of Human Femoral, Tibial, and Fibular Cortical Bone." *AM. J. ANAT*. 120, 79-88.

[14] Frankel, V.H. (1960). "The femoral neck. Function. Fracture mechanism. Internal fixation. An experimental study." Almqvist and Wiskell, Goteborg, Sweden.

[15] Funk, J.R., Rudd, R.W., Kerrigan, J.R., and Crandell, J.R. (2004). "The Effect of Tibial Curvature and Fibular Loading on the Tibial Index." *Traffic Injury Prevention*. 5, 164-172.

[16] Griffon, D.J., Wallace, L.J., and Bechtold, J. (1995). "Biomechal properties of canine corticocancellous bone frozen in normal saline solution." *Am. J. Vet. Res*. 56, 822.

[17] Hamer, A.J., Strachen, J.R., Black, M.M., Ibbotson, C.J., Stockley, I., and Elson, R.A. (1996). "Biomechanical properties of cortical allograft bone using a new method of bone strength measurement. A comparison of fresh, fresh-frozen and irradiated bone." *J. Bone Joint Surg.* 78B, 363.

[18] Kemper A, McNally C, Kennedy E, Rath A, Manoogian S, Stitzel J, and Duma S (2005): Material Properties of Human Rib Cortical Bone From Dynamic Tension Coupon Testing. *The Proc. of the*

49th International Stapp Car Crash Conference. 49, 199-230.

[19] Kuppa S,Wang J, Haffner M, Eppinger R. (2001). "Lower Extremity Injuries and Associated Injury Criteria." *Proc. 17th ESV Conf.*, Paper 457, 1–15.

[20] Linde, F., and Sorenson, H.C.F. (1993). "The effect of different storage methods on the mechanical properties of trabecular bone." *J. Biomech*. 26, 1249.

[21] McElhaney, J.H. and Byars, E.F. (1966). "Dynamic Response of Biological Materials." *ASME. Publ.* 65-WA/Huf-9.

[22] Melick, R.A., and Miller, D.R. (1966). "Variations of Tensile Strength of Human Cortical Bone with Age." *Clin. Sci*., 30, 243.

[23] Mertz HJ. (1993). Anthropometric Test Devices, in *Accidental Injury: Biomechanics and Prevention*. Ed. A. M. Nahum, J. W. Melvin, Springer-Verlag, New York, Chapter 4.

[24] Reilly, D.T., Burstien, A.H. (1975). "The Elastic and Ultimate Properties of Compact Bone Tissue." *J Biomechanics.* 8(6), 393-405.

[25] Sedlin, E.D. (1965) "A rheological model for cortical bone." *Acta Orthop. Scand*. 83, 1.

[26] Tarriere, C. and Viano, D.C. (1995). "Biomechanical Synthesis of New Data on Human Lower Leg Responses and Tolerances in Parallel with Dummies and Injury Criteria." Proceedings of the International Conference on Pelvic and Lower Extremity Injuries, 153- 160. Washington, DC: National Highway Traffic Safety Administration.

[27] Thomas, P. et al. (1995). "Lower Limb Injuries – The Effect of Intrusion, Crash Severity and the Pedals on Injury Risk and Injury Type in Frontal Collisions." Proceeding of the 39th Stapp Car Crash Conference. SAE Paper No. 952728.

[28] Weaver, J.K. (1966). "The microscopic hardness of bone." *J. Bone Joint Surg*. 48-A, 273.

[29] Welbourne ER, Shewchenko N. (1998). "Improved Measurements of Foot and Ankle Injury Risk from the Hybrid III Tibia." *Proc. 16th ESV Conf.*, Paper 98-S7-O-11, 1618–1627.

[30] Wood, J.L. (1971). "Dynamic Response of Human Cranial Bone. *J. Biomechanics*. 4, 1-12.

[31] Yamada H. (1970). "Strength of Biological Materials." Williams andWilkins Co., Baltimore, Md.

[32] Yeuheui, H.A. and Draughn, R.A. (2000). "Mechanical Testing of Bone and the Bone-Implant Interface." CRC Press LLC, New York.